

## Research Article

# Numerical Simulation of Bubble Coalescence and Break-Up in Multinozzle Jet Ejector

Dhanesh Patel,<sup>1</sup> Ashvinkumar Chaudhari,<sup>2</sup> Arto Laari,<sup>3</sup> Matti Heiliö,<sup>4</sup>  
Jari Hämäläinen,<sup>2</sup> and Kishorilal Agrawal<sup>5</sup>

<sup>1</sup>Centre for Industrial Mathematics and Department of Applied Mathematics, Faculty of Technology and Engineering, The M. S. University of Baroda, Vadodara, Gujarat 390001, India

<sup>2</sup>Centre of Computational Engineering and Integrated Design (CEID), Lappeenranta University of Technology, P.O. Box 20, 53851 Lappeenranta, Finland

<sup>3</sup>Department of Chemistry, Lappeenranta University of Technology, P.O. Box 20, 53851 Lappeenranta, Finland

<sup>4</sup>Department of Mathematics and Physics, Lappeenranta University of Technology, P.O. Box 20, 53851 Lappeenranta, Finland

<sup>5</sup>Department of Chemical Engineering, Faculty of Technology and Engineering, The M. S. University of Baroda, Vadodara, Gujarat 390001, India

Correspondence should be addressed to Dhanesh Patel; pdhanesh@yahoo.com

Received 26 October 2015; Accepted 22 December 2015

Academic Editor: Guan H. Yeoh

Copyright © 2016 Dhanesh Patel et al. This is an open access article distributed under the Creative Commons Attribution License, which permits unrestricted use, distribution, and reproduction in any medium, provided the original work is properly cited.

Designing the jet ejector optimally is a challenging task and has a great impact on industrial applications. Three different sets of nozzles (namely, 1, 3, and 5) inside the jet ejector are compared in this study by using numerical simulations. More precisely, dynamics of bubble coalescence and breakup in the multinozzle jet ejectors are studied by means of Computational Fluid Dynamics (CFD). The population balance approach is used for the gas phase such that different bubble size groups are included in CFD and the number densities of each of them are predicted in CFD simulations. Here, commercial CFD software *ANSYS Fluent 14.0* is used. The realizable  $k-\varepsilon$  turbulence model is used in CFD code in three-dimensional computational domains. It is clear that Reynolds-Averaged Navier-Stokes (RANS) models have their limitations, but on the other hand, turbulence modeling is not the key issue in this study and we can assume that the RANS models can predict turbulence of the carrying phase accurately enough. In order to validate our numerical predictions, results of one, three, and five nozzles are compared to laboratory experiments data for  $\text{Cl}_2$ -NaOH system. Predicted gas volume fractions, bubble size distributions, and resulting number densities of the different bubble size groups as well as the interfacial area concentrations are in good agreement with experimental results.

## 1. Introduction

There are number of industrial processes in which two-phase flows, that is, gas-liquid mixture, in a jet ejector are encountered. Hence, reactions occurring in gas-liquid systems are of great importance in the chemical as well as in the process industry. Mass transfers in dispersions are directly related to the mass transfer coefficients as well as the interfacial area. The jet ejector is one kind of a venturi scrubber and it is widely used for conducting gas-liquid reactions in practical applications in industry such

as pollution control and waste water treatment. Due to their simple construction, low operating cost, high energy efficiency, and good mass transfer characteristics, the jet ejectors have many advantages when used as the gas-liquid contactors. The experimental observations show that dispersed bubbles towards the bottom of the jet ejector cause highly nonuniform volume distribution in the jet ejector. The gas volume fraction, the interfacial area, and the Sauter mean bubble diameter are the three important parameters that characterize the internal flow structure of gas-liquid flows in the jet ejector [1]. The interfacial transport of mass and

momentum are proportional to the interfacial area and the driving forces. This is an important parameter required for a two-fluid model formulation [1]. The mean bubble diameter serves as a link between the gas volume fraction and the interfacial area concentration [1]. An accurate knowledge of local distributions of these three parameters is of great importance to eventual understanding and modeling of the interfacial transfer processes [1, 2]. Depending on the gas flow rate, two main flow regimes are observed in the jet ejector, namely, the homogeneous bubbly flow regime and the heterogeneous (churn-turbulent flow) regime [3]. The homogeneous regime is encountered at relatively low gas velocities and characterized by a narrow bubble size distribution and radially uniform gas holdup and it is the most desirable one for practical applications, because it offers a large contact area [2–4].

The bubble size distribution and gas holdup in gas-liquid dispersions depend extensively on the jet ejector geometry, operating conditions, and the physicochemical properties of the two phases. The design of the jet ejector has primarily been carried out by means of empirical or semiempirical correlations based mainly on experimental data. The scale-up of the jet ejector is still poorly understood due to the complexity of flow patterns and their unknown behavior under different sets of design parameters such as area ratio, projection ratio, nozzle diameter, length of free jet, throat, diffuser, convergence angle, divergence angle, and physical properties of the liquid. As a whole, the phenomenon depends strongly on the jet ejector geometry and fluid dynamics involved. It is important to note that the similar kind of study has been developed for bubble column reactor by [3].

The method to gain more knowledge and detailed physical understanding of the hydrodynamics in the jet ejector is Computational Fluid Dynamics (CFD). CFD can be regarded as an effective tool to clarify the importance of physical effects (e.g., gravity, surface tension) on flow by adding or removing them. An increasing number of papers deal with CFD applications of bubble columns [3, 5–7]. To analyze the flow pattern of the jet ejector both in steady and transient state conditions employing CFD, the majority of researchers use either two- or three-dimensional models, when numerical simulations are usually compared to experimental data. As most of the early CFD studies consider monodispersed bubble size distributions ignoring break-up and coalescence mechanisms, their validity is limited [3].

During the last two decades, significant developments have been done in the modeling of two-phase flow processes because of the introduction of the two-fluid models [1]. In the two-fluid models, the interfacial transfer terms are related to the interfacial area concentration and the degree of turbulence near the interfaces [1]. Since the interfacial area concentration represents the key parameter that links the interaction of the phases, significant attention has been paid towards developing a better understanding of the coalescence and breakage effects due to interactions among bubbles and between bubbles and turbulent eddies for gas-liquid bubbly

flows [1, 2, 7–11]. The population balance method is a well-known method for tracking the size distribution of the dispersed phase and accounting for the breakage and coalescence dynamics in bubbly flows [1, 12–22]. The population balance method was also used by Hämäläinen et al. [23] and Hämäläinen [24] in paper industry for papermaking suspension flow.

In gas-liquid two-phase systems, bubble break-up and coalescence can greatly influence their overall performance by altering the interfacial area available for the mass transfer between the phases [3]. Therefore, in order to develop reliable predictive tools for designing the jet ejectors, it is essential to obtain some insight into the prevailing phenomena through simulation models based on the bubble formation and distraction mechanisms, that is, bubble coalescence and break-up [3, 12, 15, 25–28], incorporated into CFD simulation making it possible to calculate hydrodynamic variables such as liquid velocity, gas holdup, and bubble size distributions.

In this work, an attempt has been made to demonstrate the possibility of combining the population balance models with Computational Fluid Dynamics (CFD) for the case of a gas-liquid bubbly flow in the jet ejector. In all these processes gas holdup,  $\varepsilon_g$ , and bubble size distribution are important design parameters, since they define the gas-liquid interfacial area available for interfacial area mass transfer ( $a$ ), which is given by

$$a = \frac{6\varepsilon_g}{d_{32}}, \quad (1)$$

where  $d_{32}$  is the mean Sauter diameter of the bubble size distribution [3]. The MUSIG model implemented in *ANSYS Fluent 14.0*, which accounts for the nonuniform bubble size distribution in a gas-liquid flow [1, 2, 6, 16, 29], is used in this paper. Gas volume fraction, bubble size distribution, number density of bubbles, gas and liquid pressure variation, interfacial area concentration, and gas and liquid velocity variation in jet ejector are predicated. The flow pattern development has been studied at the free jet end, and at the throat end, and at the end of the ejector in detail. In addition, numerical predictions are compared with experiments and the predicated gas interfacial area is in a good agreement with experimental results.

## 2. Jet Ejector

A large choice of gas-liquid contactors, for example, the falling film column, spray column, packed column, plate column, bubble column, mechanically agitated contactors, spray towers, and venturi scrubbers, are available for understanding the mass transfer process. Among these, the venturi scrubber is a wet type design for gas-liquid contactors. In venturi type of scrubber

- (i) liquid is a medium to absorb objectionable gases and particulates from industrial gaseous waste streams;

- (ii) a high velocity section of fluid jet is utilized to bring the liquid and gas into intimate contact with each other.

Venturi scrubbers fall into two categories [30, 31].

In the first category, it uses mechanical blower to draw a high velocity gas stream through the system. The liquid was originally at rest but once the gas accelerates, it splits into droplets. Particulates and gases are then confined into the comparatively slower moving droplets. This type is called a “high energy venturi scrubber” (HEVS). The scrubbing liquid can be introduced in two ways:

- (i) If the liquid is introduced through nozzles which is usually at the throat it is known as Pearce-Anthony venturi scrubber.
- (ii) In this case liquid is introduced as a film which is usually known as the wetted approach type.

Secondly, a mechanical pump or compressor is used to generate a high velocity to the liquid/fluid jet. This liquid/fluid jet creates suction and gas is entrained into it by transfer of momentum. This type of the venturi scrubber is called an ejector venturi scrubber or “jet ejector.”

The jet ejectors have some advantages over other types of contactors which are mentioned as follows [31, 32]:

- (i) Lower initial capital cost.
- (ii) Simple construction and being compact.
- (iii) Easy installation and operation.
- (iv) No moving parts, so little chances of mechanical failure and hence highly reliable.
- (v) Being able to deal with wet, hot, and corrosive gases and thick, aggressive, and inflammable particles.
- (vi) Ability to separate gaseous pollutant and fine particulate matter simultaneously.
- (vii) Being able to handle large gas flow rates.
- (viii) High heat and mass transfer rates and interfacial area.

However, it is not energy efficient equipment as a fluid moving device. But it has been reported that it has high efficiency as a gas-liquid contacting device [33–36].

The jet ejectors are especially effective in chemical and biochemical industries for gas purification and for collaborating gas-liquid reactions like chlorination, oxidation, hydrogenation, and hydroformulation processes. Jet ejectors use high kinetic energy of the operating fluid jet to promote break-up and distribution of the suction fluid into small droplets/bubbles and to pull the gas through the system and push through the connected outlet.

A typical gas-liquid jet ejector is displayed in Figure 1. It consists of a converging section, a throat section, and a diffuser/divergent section. The gas is accelerated to atomize the scrubbing liquid in the convergent section to reach a higher velocity in the throat. Throat is used for interaction of liquid and gases. In the diffuser/divergent section the gas is slowing down allowing some recovery of pressure [37, 38].

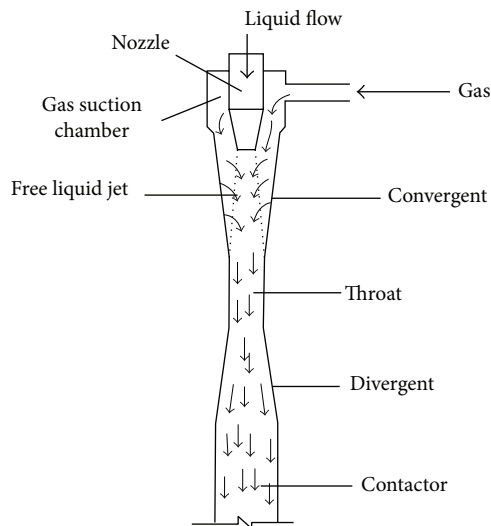


FIGURE 1: Typical gas-liquid jet ejector [31, 113].

Jet ejectors have favorable mixing and mass transfer characteristics so they are more used among other gas-liquid contactors. A jet ejector is a device in which suction, mixing, and dispersal of secondary fluid take place and are based on the principle of utilizing the kinetic energy of a high velocity motive (primary) fluid jet to entrain the secondary phase to create fine dispersion of two phases (Utomo et al. [39]). The secondary fluid may be dispersed by the shearing action of the high velocity motive fluid or motive fluid may get dispersed when it is captured by a secondary fluid [40].

Figure 1 shows the typical ejector system in which the jet of primary fluid, typically liquid, is pumped into the system through high velocity through a nozzle flowing out of a nozzle which creates a low pressure region in the suction chamber, into which secondary fluid, typically gas, moves according to Bernoulli's principle. The driving force for entrainment of the secondary fluid is developed due to the pressure difference between the entry point of the secondary fluid and the nozzle tip. There is a mixing of gas and liquid phases and a gas-liquid dispersion takes place in the mixing tube. In the diffuser the pressure is recovered. Coaxial-flow and froth-flow are the two principal flow regimes in jet ejectors. In the annular region formed between the jet of primary fluid and ejector wall, a central core of primary fluid with secondary fluid flowing was observed. This regime forms coaxial-flow. Froth-flow consists of liquid in which gas phase is completely dispersed in the form of bubble [41]. The phenomenon of change from coaxial-flow to froth-flow is termed as mixing shock [42]. The small bubbles are generated due to mixing shock which turns into creation of large interfacial area ( $\sim 2000 \text{ m}^2/\text{m}^3$ ). Therefore greater rates of reaction and superior gas-liquid mass transfer rates are obtained in ejectors, in comparison to other common gas-liquid contactors [31].

Depending on application, there may be different objectives for design of an ejector which are as follows [43]:

- To achieve greater entrainment of the secondary fluid.
- To yield deep mixing between the two fluids.
- To inject fluids from a region of low pressure to a region of higher pressure.

Jet ejector may be used as a vacuum producing device as well as jet pump. With the rapid growth of the chemical process industry, their use as entraining and pumping corrosive liquids, slurries, fumes, and dust-laden gases has increased. Their use as mass transfer equipment for liquid-liquid extraction, gas absorption, gas stripping, and slurry reaction, like hydrogenation, oxidation, chlorination, fermentation, and so forth, has increased [31, 44–53].

The numbers of researchers have attempted to optimize performance of jet ejector [40, 51, 54–71] due to its increasing growth rate in usage. Many researchers have studied the mass transfer characteristics and performance of the jet ejectors followed by contactors, draft tube, packed column, or bubble column and they have similar conclusion that there is less mass transfer coefficient in the extended portion in comparison to the ejector [31, 34, 39, 56, 69–87]. Dutta et al. [74] and Gamisans et al. [60] studied the jet ejectors and observe that jet ejector without diffuser or throat is less effective in comparison to ejector with them. Das and Biswas [40] observe that efficiency of ejector depends on the design of the suction chamber, the throat, the diffuser, and the nozzle. Apart from the dimensions of the various sections of the ejector, the factors such as shape of the entrance to the parallel throat, shape of entry of convergent section, throat aspect ratio, angle of divergence and convergence, and the projection ratio are also important factors to be reflected. Various researchers have studied the effect of geometry of jet ejector in the optimal design of jet ejector. Also, many researchers have worked on flow patterns in jet ejector (see [79, 88–92]).

Performance of jet ejector is also depending on the factors like bubble size distributions, correlation for entrainment, bubble diameter, drag force, and gas holdup and factors affecting the bubble size. Measurement of bubble size is critical issue. The researchers in these directions are Lefebvre [93], Liu [94], Schick [95], Xianguo and Tankin [96], Dennis Gary [97], Azad and Syeda [98], Frank [88], Silva et al. [99], Kudzo [100], Ciborowski and Bin [101], Ohkawa et al. [102], Sheng and Irons [103], Kitscha and Ocamustafaogullari [104], Bailer [105], Evans et al. [106], Ceylan et al. [107], Havelka et al. [76], Mandal et al. [81], Zahradník and Fialová [90], Bailer [105], Pawelczyk and Pindur [108], Dutta and Raghavan [74], Biń [109], and Zheng et al. [110].

Figure 2 shows the major parts like primary fluid inlet, secondary fluid inlet, suction chamber, converging section, throat/mixing zone, and diverging section/diffuser of an ejector. The symbols which we have used for describing different components are as follows:

- Length of throat ( $L_T$ ), length of diffuser ( $L_D$ ), and distance between nozzle and commencement of throat ( $L_{TN}$ ).
- Diameter of nozzle ( $D_N$ ), diameter of throat ( $D_T$ ), and diameter of suction chamber ( $D_S$ ).

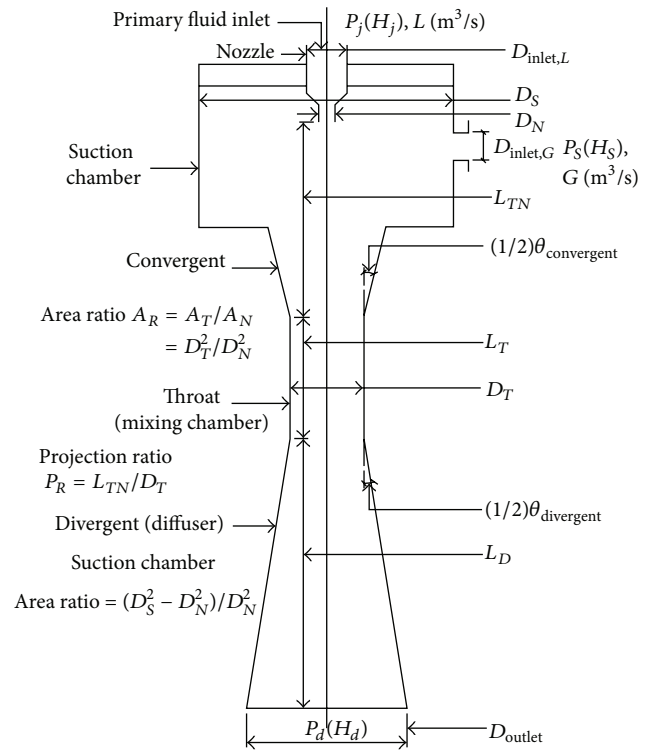


FIGURE 2: Schematic diagram showing geometry of an ejector [31, 111, 112].

- Area of throat ( $A_T$ ), area of nozzle ( $A_N$ ), and area of suction ( $A_S$ ).
- Angle of converging sections ( $\theta_{\text{convergent}}$ ) and angle of diverging sections ( $\theta_{\text{divergent}}$ ).

Performance of the ejectors has been studied in terms of

- area of throat/area of nozzle, that is, area ratio ( $A_R = A_T/A_N$ ),
- length of throat/diameter of throat, that is, throat aspect ratio ( $L_T/D_T$ ),
- distance between nozzle tip and the commencement of throat/diameter of throat, that is, projection ratio ( $P_R = L_{TN}/D_T$ ),
- suction chamber area ratio ( $A_S/A_N = (D_S^2 - D_N^2)/D_N^2$ ).

### 3. Mathematical Model

The poly dispersed multiphase flow is observed in jet ejector. It means that the dispersed phase covers a wide range of size groups. One of the characteristics of this flow is that the different sizes of the dispersed phase interact with each other through the processes of break-up and coalescence. A population balance equation is framed to deal with this kind of a flow. It is well known that the population balance model is best fitted method to calculate the size distribution of a dispersed phase which includes break-up and coalescence effect [3]. Our model is in parallel to the model developed by

Mouza et al. [3]. The general form of the population balance equation is

$$\frac{\partial n_i}{\partial t} + \nabla \cdot (\tilde{u}_g n_i) = b_B - d_B + b_C - d_C, \quad (2)$$

where  $n_i$ ,  $b_B$ ,  $d_B$ ,  $b_C$ ,  $d_C$ , and  $\tilde{u}_g$  represent the number density of size group  $i$ , the birth rate due to break-up, the death rate due to break-up, the birth rate due to coalescence, the death rate due to coalescence, and the gas velocity, respectively. The relation between number density  $n_i$  and the volume fraction  $\alpha_g$  is given by

$$\alpha_g f_i = n_i V_i, \quad (3)$$

where  $f_i$  and  $V_i$  represent the volume fraction and the corresponding volume of a bubble of group  $i$ , respectively. The coalescence of two bubbles occurs in three steps [3, 19]:

- (i) First, the bubbles collide trapping a slight amount of liquid between them.
- (ii) Secondly, this liquid film drains until it reaches a critical thickness.
- (iii) At the end, the film breaks and the bubbles join together.

The process of coalescence depends on the collision rate of the two bubbles and the collision efficiency. Coalescence is a function of  $t_{ij}$  and  $\tau_{ij}$ , where  $t_{ij}$  is the time required for coalescence and  $\tau_{ij}$  is the contact time. Collision is as a result of turbulence ( $\theta_{ij}^{Tu}$ ), laminar shear ( $\theta_{ij}^{Ls}$ ), and buoyancy ( $\theta_{ij}^{By}$ ). The total coalescence rate is

$$Q_{ij} = (\theta_{ij}^{Tu} + \theta_{ij}^{Bu} + \theta_{ij}^{Ls}) e^{-t_{ij}/\tau_{ij}}. \quad (4)$$

Collision is also developed due to the difference in rise velocities of bubbles with different sizes. The two conditions observed in jet ejector in parallel to the work of Mouza et al. [3] for bubble column are as follows:

- (i) Jet ejectors operate at the homogeneous regime. Due to the narrow bubble size distribution in homogeneous regime, the relative effect of buoyancy can be neglected which leads to the assumption that bubbles rise with the same velocity regardless of their size.
- (ii) Collision occurs as a result of strong circulation pattern in jet ejector. However this happens at gas rates higher than those encountered in the homogeneous regime and hence laminar shear term may be neglected.

Hence, there is only the turbulent contribution in the model which is given by

$$\theta_{ij}^{Tu} = n_i n_j S_{ij} (\bar{u}_{ti}^2 + \bar{u}_{tj}^2), \quad (5)$$

where  $n_i$ ,  $n_j$ , and  $\bar{u}_i$  are the concentrations of bubbles of radius  $r_{bi}$ , concentrations of bubbles of radius  $r_{bj}$ , and the average turbulent fluctuating velocity, respectively. The collision

cross-sectional area ( $S_{ij}$ ) of the bubble, the time required for coalescence, and the contact time are given by (6), (7), and (8), respectively:

$$S_{ij} = \frac{\pi}{4} (R_{bi} + R_{bj})^2, \quad (6)$$

$$t_{ij} = \left( \frac{R_{ij}^3 \rho_l}{16\sigma} \right)^{0.5} \ln \frac{h_0}{h_f}, \quad (7)$$

$$\tau_{ij} = \frac{R_{ij}^{2/3}}{\varepsilon^{1/3}}, \quad (8)$$

where  $R_{ij}$ ,  $\rho_l$ ,  $\sigma$ ,  $\varepsilon$ ,  $h_0$ , and  $h_f$  are the equivalent radius, the density of the liquid phase, the surface tension, the turbulent energy dissipation, the film thickness when collision begins, and the film thickness when ruptures of the film occur, respectively. The birth rate of group  $i$  due to coalescence of group  $k$  and group  $j$  bubbles and the death rate of group  $i$  due to coalescence with other bubbles are given by (9) and (10), respectively:

$$b_C = \frac{1}{2} \sum_{j=1}^i \sum_{k=1}^i Q_{jk} n_j n_k, \quad (9)$$

$$d_C = n_i \sum_{j=1}^N Q_{ij} n_j. \quad (10)$$

The break-up of bubbles in turbulent dispersions employs the model developed by Luo and Svendsen [28]. The break-up rate of bubbles of size  $i$  into bubbles of size  $j$  is given by

$$g(v_j : v_i) = 0.923 (1 - \alpha_g) \sqrt[3]{\left( \frac{\varepsilon}{d_j^2} \right)} \int_{\mu_{\min}}^1 \frac{(1 + \mu)^2}{\mu^{11/3}} e^{-\tau_c} d\mu, \quad (11)$$

where  $\varepsilon$ ,  $d_j$ ,  $\mu$ ,  $\tau_c$ , and  $N$  represent the turbulent energy dissipation rate, the bubble diameter, the dimensionless size of eddies in the inertial subrange of isotropic turbulence, the critical dimensionless energy for break-up, and the total number of groups, respectively.

The birth rate of group  $i$  bubbles due to break-up of larger bubbles and the death rate of group  $i$  bubbles due to break-up into smaller bubbles are given by (12) and (13), respectively:

$$b_B = \sum_{j=i+1}^N g(v_j : v_i) n_j, \quad (12)$$

$$d_B = g_i n_i. \quad (13)$$

The mass conservation equation for the liquid phase, the mass conservation equation for the gas phase, and the momentum

conservation equation in the Eulerian framework are given by (14), (15), and (16), respectively:

$$\frac{\partial(\alpha_i \rho_i)}{\partial t} + \nabla \cdot (\alpha_i \rho_i \vec{u}_i) = 0, \quad (14)$$

$$\frac{\partial(\alpha_g f_i \rho_g)}{\partial t} + \nabla \cdot (\alpha_g f_i \rho_g \vec{u}_g) = S_i, \quad (15)$$

$$\begin{aligned} & \frac{\partial(\alpha_m \rho_m \vec{u}_m)}{\partial t} + \nabla \\ & \cdot (\alpha_m \rho_m \vec{u}_m \vec{u}_m - \mu_m \alpha_m (\nabla \vec{u}_m + (\nabla \vec{u}_m)^T)) \\ & = -\alpha_m \nabla p + M_{mn} + \rho_m g, \end{aligned} \quad (16)$$

where  $\rho_m$ ,  $\vec{u}_m$ ,  $\alpha_m$ ,  $\mu_m$ ,  $p$ ,  $M_{mn}$ , and  $g$  represent the density, the velocity, the volume fraction, and the viscosity of the  $m$ th phase, the pressure, the interphase momentum exchange between phase  $m$  and phase  $n$ , and the gravitational force, respectively.

The momentum exchange between gas and liquid phase is given by

$$M_{lg} = \frac{3}{4} \rho_m \frac{\alpha_g}{d_{32}} C_D (\vec{u}_g - \vec{u}_l) |\vec{u}_g - \vec{u}_l|, \quad (17)$$

where  $C_D$  is the interfacial drag coefficient.

#### 4. Simulation Parameter for Jet Ejector Geometry

Figure 3 shows the details of the geometry of ejector. Agrawal [31, 111, 112] has done the experiments based on the experimental setup as shown in Figure 4. It is important to note that these experiments were conducted on the industrial stage ejector. Data for the geometry of the ejector is shown in Table 1.

#### 5. The CFD Simulation

Accurate modeling of the jet ejector requires a Population Balance Modeling (PBM) to be solved simultaneously with a CFD solver because of the presence of bubble-bubble contacts or bubble-liquid contacts. The PBM-CFD model, that is, MUSIG model (*ANSYS Fluent 14.0*), is implemented in this study which combines the population balance method with the break-up [28] and coalescence [19] models in order to predict the bubble size distribution of the gas phase. This model uses the Eulerian-Eulerian model. The MUSIG model has been extensively used for different systems [1–3, 11, 16, 20, 27, 29].

The equations of continuity, momentum, and turbulence for the continuous and dispersed phases give a standard two-phase flow calculation. It can be extended to include number density of bubbles within several size groups using the MUSIG model.

The size range of the bubbles is split into several groups with, for example, groups of equal diameter. Equations are

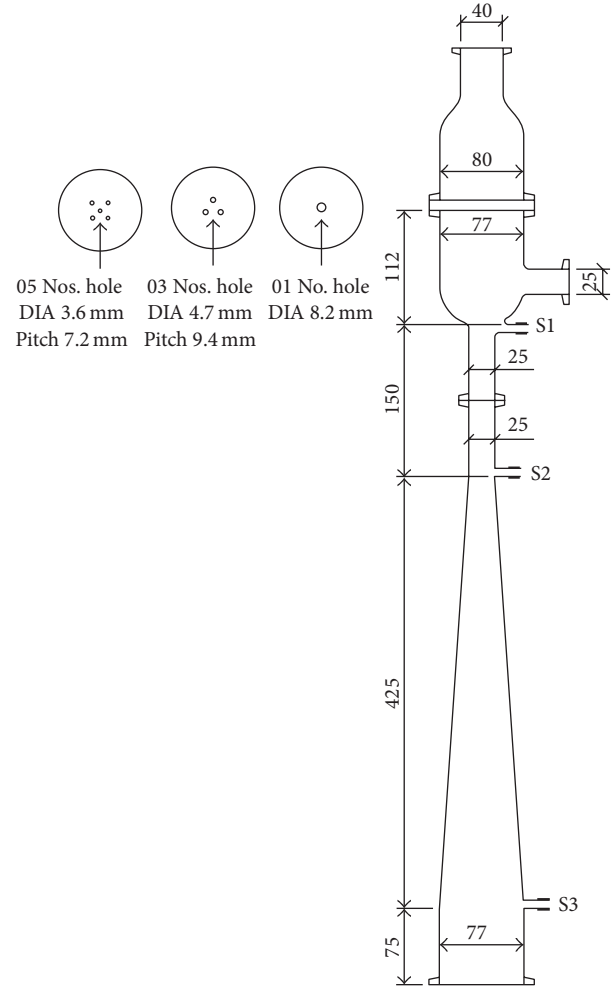


FIGURE 3: Detail of the ejector used in the experimental setup [31, 111, 112].

then solved for the number density in each group. These size fractions provide a more accurate measure of the interfacial area density.

In this study, the simulation is done in three dimensions and three geometries of the ejector, namely, with one nozzle, three nozzles, and five nozzles, as described in Figure 3. In the present study, bubbles ranging from  $1.4472692 \times 10^{-5}$  m (bin-20) to  $9.7005842 \times 10^{-4}$  m (bin-0) in diameter are equally divided into 21 classes (see Table 2) as the experimental observation of the gas volume fraction is 100% and therefore we consider 0.005, 0.010, 0.015, 0.018, 0.020, 0.025, 0.032, 0.030, 0.035, 0.040, 0.045, 0.050, 0.055, 0.060, 0.065, 0.070, 0.075, 0.080, 0.085, 0.090, 0.095, and 0.100 which represent the volume fraction of the bubbles of group  $i$ , ( $i = 0, 1, 2, 3, 4, 5, \dots, 20$ ). In view of computational time's resources, we consider the subdivision of the bubble sizes into 21 size groups. All computational results are based on the discretization of the bubble sizes into 21 groups. *ANSYS Fluent 14.0* gives solution to the coupled sets of governing equations for the balances of mass and momentum of each phase. The conservation equations were discretized using the control volume technique. Similar kind of study

TABLE I: Dimensions of ejector [31, 111, 112].

		Setup-III		
Nozzle diameter	$D_N$	8.2 mm	4.7 mm	3.7 mm
Number of nozzles	$n$	1	3	5
Nozzle number		5	6	7
Pitch*			$2D_N$	
Area ratio (appx.)**	$A_R$		9.3	
Diameter of throat/mixing tube	$D_T$		25 mm	
Length of throat/mixing tube***	$L_T$		150 mm	
Projection ratio#	$P_R$		4.5	
Angle of convergence	$\theta_{con}$		Well rounded	
Angle of divergence of conical diffuser##	$\theta_{div}$		$7^\circ$	
Length of the conical diffuser	$L_d$		425	
Diameter of the diffuser exit	$D_C$		77	
Diameter of extended contactor	$D_C$		(—)	
Length of extended contactor	$L_C$		(—)	
Diameter of the suction chamber	$D_S$		77 mm	
Length of the suction chamber	$L_S$		122 mm	
Distance between nozzle & commencement of throat	$L_{TN}$		112 mm	
Diameter of secondary gas inlet	$D_{G,In}$		25 mm	
Volume of free jet	$V_C$		$26.32 \times 10^{-6} \text{ m}^3$	
Volume of throat	$V_T$		$73.6 \times 10^{-6} \text{ m}^3$	
Volume of divergence	$V_D$		$1156.78 \times 10^{-6} \text{ m}^3$	
Total ejector volume	$V_J$		$1256.7 \times 10^{-6} \text{ m}^3$	

\* Panchal et al. [114], \*\* Acharjee et al. [54], \*\*\* Biswas et al. [57], # Yadav and Patwardhan [43], and ## Mukherjee et al. [65].

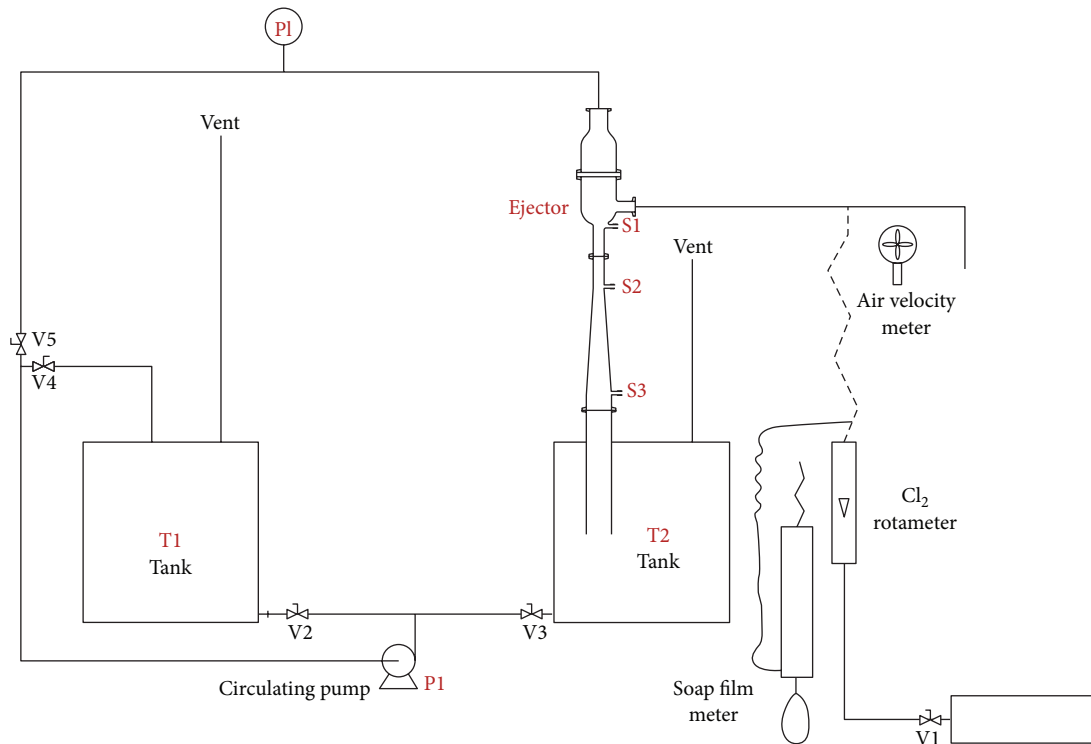


FIGURE 4: Schematic diagram of the experimental setup [31, 111, 112].

TABLE 2: Diameter of each bubble class tracked in the simulation.

Bubble diameter, $d_i$ (m) (bin size)	Class index (bin number)
$9.7005842 \times 10^{-4}$	Bin-0-fraction
$7.8611387 \times 10^{-4}$	Bin-1-fraction
$6.3704928 \times 10^{-4}$	Bin-2-fraction
$5.1625064 \times 10^{-4}$	Bin-3-fraction
$4.1835809 \times 10^{-4}$	Bin-4-fraction
$3.3902814 \times 10^{-4}$	Bin-5-fraction
$2.747409 \times 10^{-4}$	Bin-6-fraction
$2.2264395 \times 10^{-4}$	Bin-7-fraction
$1.802573 \times 10^{-4}$	Bin-8-fraction
$1.4621301 \times 10^{-4}$	Bin-9-fraction
$1.1848779 \times 10^{-4}$	Bin-10-fraction
$9.6019883 \times 10^{-5}$	Bin-11-fraction
$7.7812388 \times 10^{-5}$	Bin-12-fraction
$6.3057437 \times 10^{-5}$	Bin-13-fraction
$5.1100352 \times 10^{-5}$	Bin-14-fraction
$4.1410594 \times 10^{-5}$	Bin-15-fraction
$3.3558229 \times 10^{-5}$	Bin-16-fraction
$2.7194846 \times 10^{-5}$	Bin-17-fraction
$2.2038101 \times 10^{-5}$	Bin-18-fraction
$1.7859189 \times 10^{-5}$	Bin-19-fraction
$1.4472692 \times 10^{-5}$	Bin-20-fraction

TABLE 3: Operating conditions.

Gas phase	Air plus chlorine at 25°C
Liquid phase	Water plus sodium hydroxide at 25°C
Average gas volume fraction	1.0

can be found from Mouza et al. [3] and Ekambara et al. [1].

The simulations have been carried out for nozzle 1 by using 7,22,021 tetrahedral cells, 1,37,3357 triangular interior faces, 1,40,779 triangular wall faces, 430 triangular pressure-outlet faces, 161 triangular velocity-inlet faces, and 156,799 nodes. The simulations have been carried out for nozzle 3 by using 7,23,519 tetrahedral cells, 1,37,6107 triangular interior faces, 1,41,271 triangular wall faces, 430 triangular pressure-outlet faces, 161 triangular velocity-inlet faces, and 157,190 nodes. The simulations have been carried out for nozzle 5 by using 7,15,031 tetrahedral cells, 1,35,9401 triangular interior faces, 1,40,731 triangular wall faces, 430 triangular pressure-outlet faces, 161 triangular velocity-inlet faces, and 155,599 nodes.

A second-order discretization scheme was used for the convective terms. At the inlet, gas, liquid, and the average volume fraction have been specified. At the outlet, a relative average static pressure of zero was specified. The operating conditions are summarized in Table 3. The fluid data are taken at room temperature (25°C).

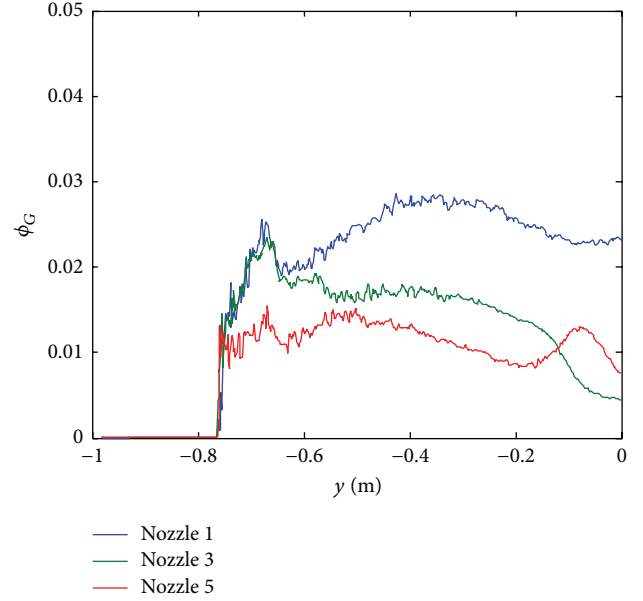


FIGURE 5: Plot of the volume fraction of gas.

## 6. Results and Discussion

In this work, we have made an effort to study Chlorine-Aqueous Sodium Hydroxide system. As stated earlier, the bubble sizes were distributed into twenty groups (bins) with diameters between  $1.4472692 \times 10^{-5}$  m and  $9.7005842 \times 10^{-4}$  m.

**6.1. Gas Volume Fraction and Liquid Volume Fraction.** Figures 5 and 6 show the plot of the predicted gas volume fraction and predicted liquid volume fraction for liquid velocities of 4.6 m/s and gas velocity of 0.2866 m/s for nozzles 1, 3, and 5, respectively. It can be observed that most of the gas volume fraction tends to migrate towards the bottom of the ejector. It is also observed that the gas volume increases in the area of the throat as well as near the gas inlet. As the number of nozzles increases (from nozzle 1, to nozzle 3, to nozzle 5), the gas volume fraction decreases with the same trend in all the nozzles. As we proceed from nozzle to end of jet ejector we are not adding any gas or liquid so it should be parallel to axis. There are three clear cut zones (a) from discharge of liquid nozzle to beginning of the throat, (b) from commencement to the end of the throat, and (c) from end of the throat to end of the diffuser. In zone (a) there is a negative pressure so same quantity of gas has more volume at constant temperature which is clear by peak zone. In the throat there is almost constant pressure which is shown as almost parallel line in this zone. The volume fraction of gas should reduce since the pressure is recovered and higher in zone (c). This fact is evident from Figure 5 as the volume fraction of gas is slanting downward.

**6.2. Liquid Velocity and Gas Velocity.** Figures 7 and 8 represent the plots of the velocity magnitude of the gas and liquid phases, respectively. These results show that the axial liquid

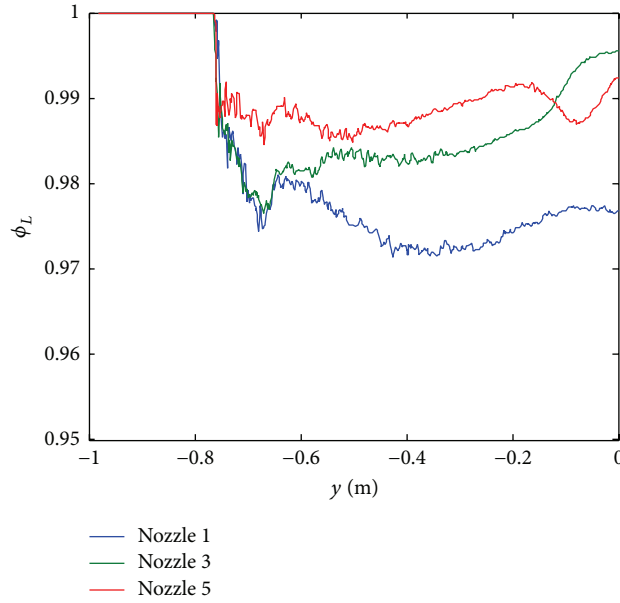


FIGURE 6: Plot of the volume fraction of liquid.

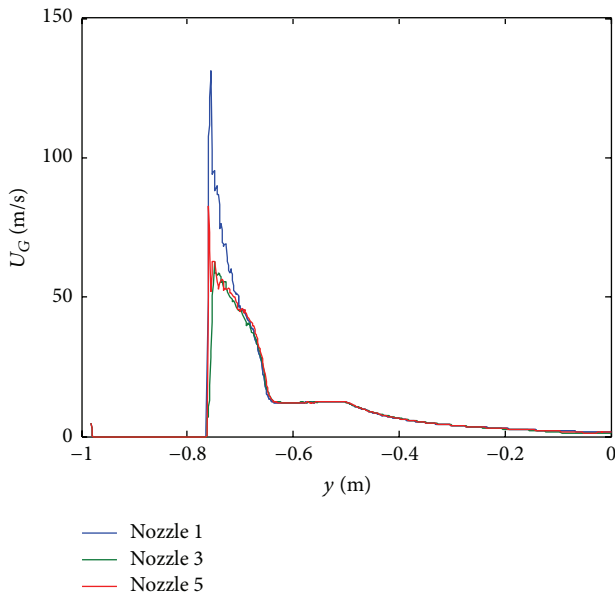


FIGURE 7: Plot of the velocity magnitude of gas.

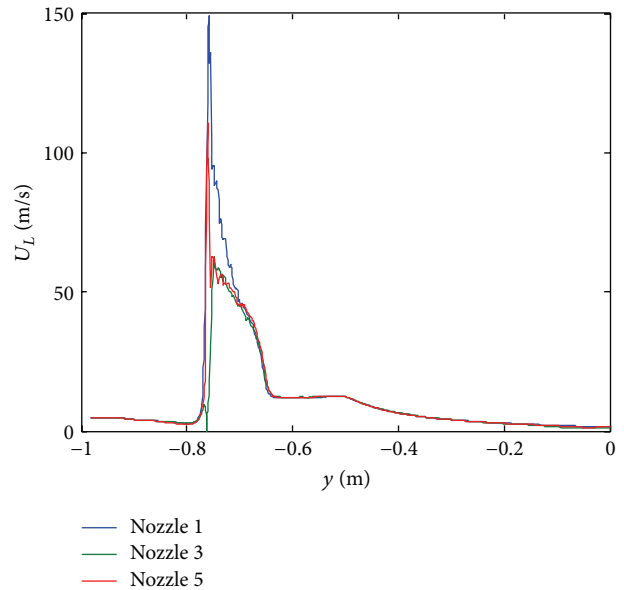


FIGURE 8: Plot of the velocity magnitude of liquid.

velocity profile has a slight degree of asymmetry due to the presence of the gas flow. The liquid velocity in the upper region of the jet ejector is higher than in the lower region. This is due to the increase in cross-sectional area at the bottom of the ejector.

**6.3. Bubble Size Distribution.** Bubble coalescence and break-up determine the bubble size distribution. Gas volume fraction and the kinetic energy dissipation rate influence the bubble coalescence and break-up in jet ejector. The bubble

size distribution varies with the position because of the nonuniform profiles of the gas volume fraction entrapped by liquid stream and dissipation rate (see [1, 3]). The number densities of the bubbles along the vertical direction which is middle line of the jet ejector for bin-0, bin-10, and bin-20 are shown in Figures 10, 12, and 14, respectively, for liquid velocities of 4.6 m/s and gas velocity of 0.2866 m/s. Similarly the number densities of the bubbles in vertical middle plane of the jet ejector for bin-0, bin-10, and bin-20 are shown in Figures 9, 11, and 13, respectively. It is observed that the bubble size having more diameters is at the end. In zones (a) and

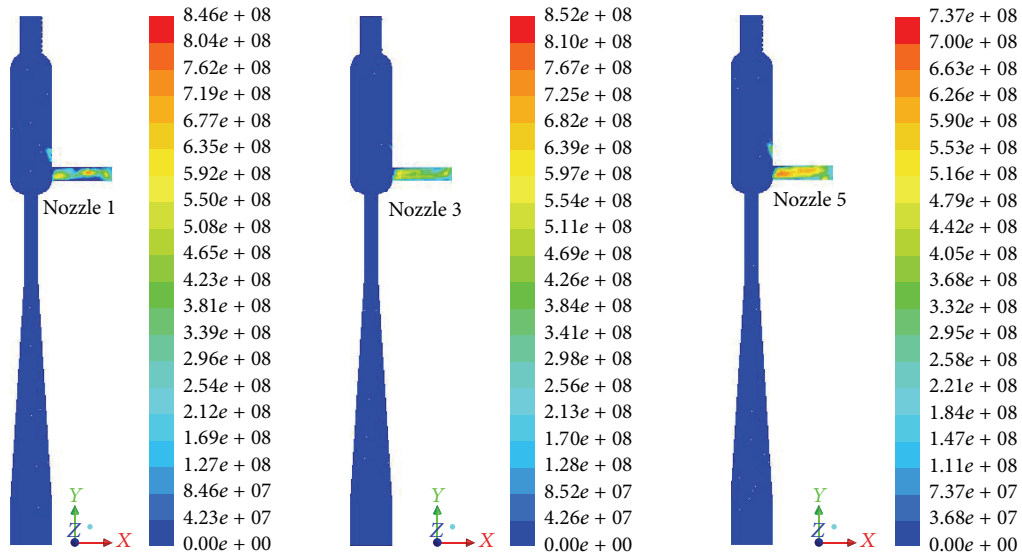


FIGURE 9: Contour of the number density of bin fraction 0 for nozzles 1, 3, and 5.

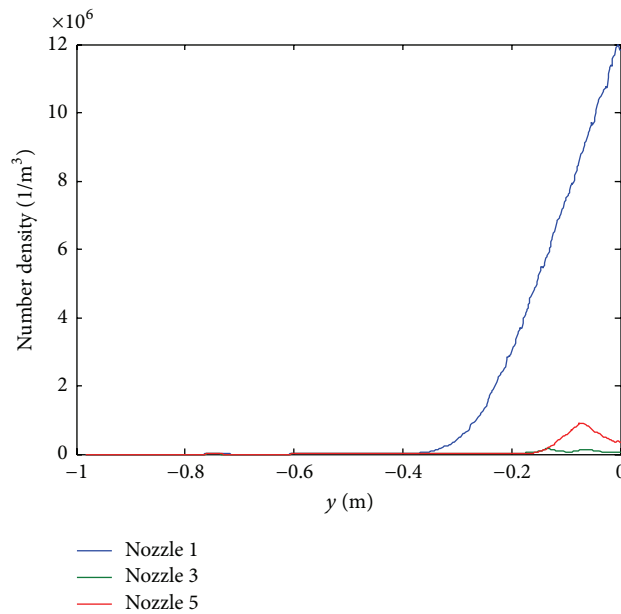


FIGURE 10: Plot of the number density of bin fraction 0.

(b), the bubble size reduces due to the intimate mixing. It can be seen from these figures that the bubble size distribution function reaches an independent state as determined by the balance between birth and death processes that depend on the local flow conditions.

Figures 15–17 represent the discrete number density of the bubbles for nozzles 1, 3, and 5, respectively, for the entire volume. Figures 18–20 represent the discrete number density of the bubbles for nozzles 1, 3, and 5, respectively, for the plane near to gas inlet. It is evident from the figure that as the

diameter increases the number density decreases for entire volume as well as the plane near to throat.

**6.4. Interfacial Area.** The present simulation results show the interfacial area variation along the vertical direction which is middle line of the jet ejector as shown in Figure 22. The variation of interfacial area in vertical middle plane is also shown in Figure 21. From Figures 5 and 22, it can be seen that the appearance of interfacial area concentration looks

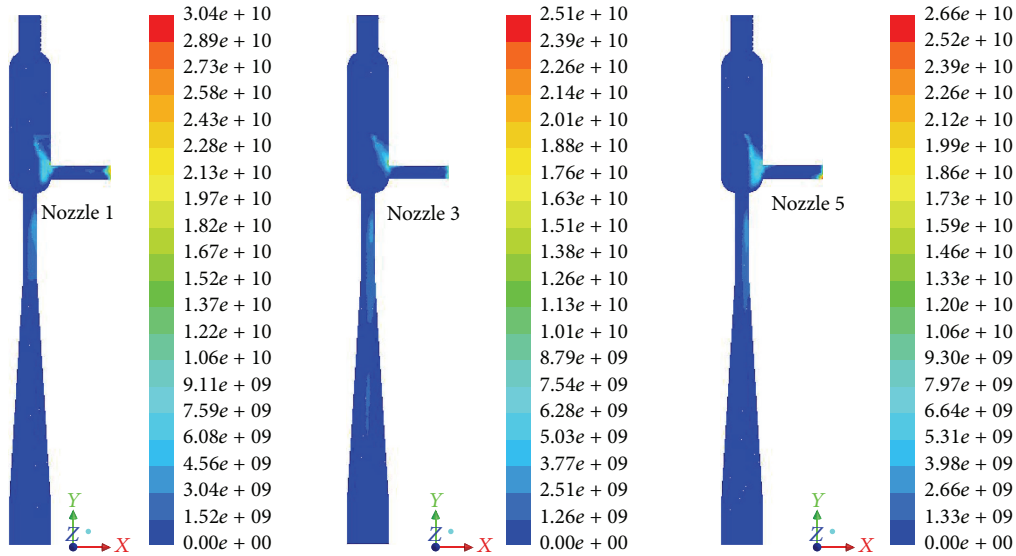


FIGURE 11: Contour of the number density of bin fraction 10 for nozzles 1, 3, and 5.

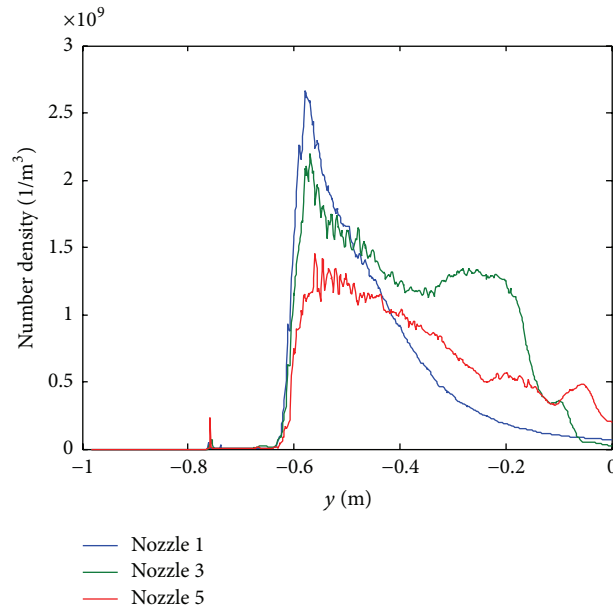


FIGURE 12: Plot of the number density of bin fraction 10.

similar to the gas volume fraction. But the interfacial area is depending not only on the volume fraction of the gas, but also equally on the distribution of the bubble size. Since the measurements of the volume fraction and the interfacial area are independent of each other, the data required for calculating an interfacial area from population balance model provides a valuable test for model prediction [1, 3]. Hence our results show that the birth and the death processes modeled in the population balance model are appropriate to describe the dynamics of bubbles. It can be also seen that the interfacial area concentration reaches the maximum value of  $7000 \text{ m}^2/\text{m}^3$ ,  $5600 \text{ m}^2/\text{m}^3$ , and  $4500 \text{ m}^2/\text{m}^3$  in the mixing zone of the jet ejector for the nozzles 1, 3, and 5, respectively.

It is also observed that the interfacial area is decreasing when the number of nozzles is increased. The interfacial area is in good agreement with experimental result [31].

The range of measured values of the interfacial area in the jet ejector is about  $3000$  to  $13000 \text{ m}^2/\text{m}^3$  [31]. The experimental values of the interfacial area for nozzle 1, nozzle 3, and nozzle 5 are nearly in the range of  $4000$ – $5500 \text{ m}^2/\text{m}^3$ ,  $3800$ – $4500 \text{ m}^2/\text{m}^3$ , and  $2500$ – $3500 \text{ m}^2/\text{m}^3$ , respectively, for different concentrations of gas and liquid [31]. The simulated values of the interfacial area concentration are in the same order of magnitude with the experimental results [31]. More detail on the experimental results can be found in Agrawal [31].

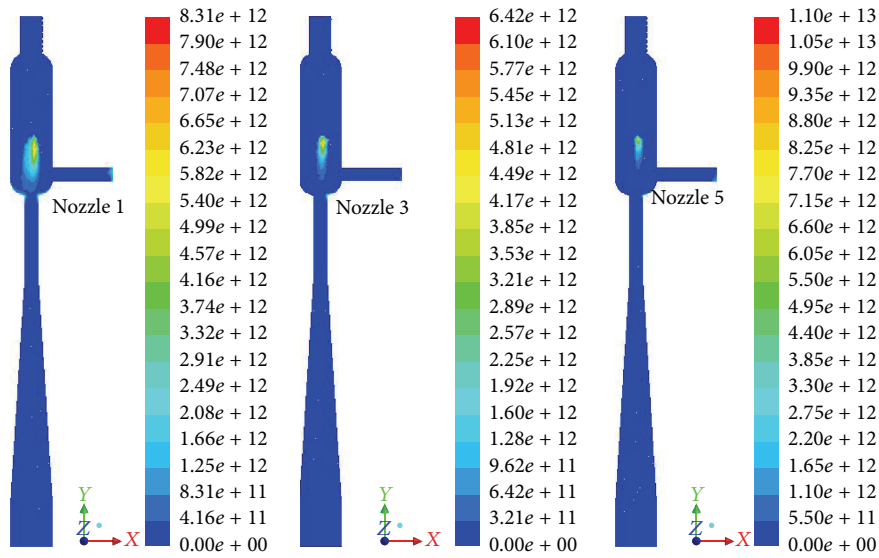


FIGURE 13: Contour of the number density of bin fraction 20 for nozzles 1, 3, and 5.

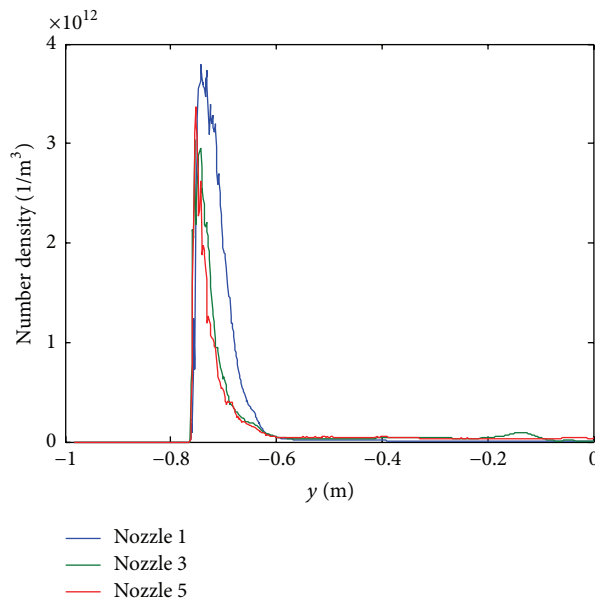


FIGURE 14: Plot of the number density of bin fraction 20.

As shown in Figure 23, the correlation shows that diameter is less in zone (a) but increases in zone (b) and is almost constant in zone (c). In zone (c) there is sudden rise of the diameter in the case of nozzle 1, whereas in the cases of nozzles 3 and 5 the diameter does not show appreciable change. The reason is that in nozzle 1 there is only single jet. Its singularity nature is not disturbed while fluids are passing through the jet ejector. Hence there is fast collision of bubbles and it shows sudden rise in the bubble diameter, while, in the cases of nozzles 3 and 5, the water jet is divided into

three and five jets of the same velocity, respectively, so these streams maintain their diversity. While fluid stream enters into the diffuser, the bubbles entrapped in streams are not easily disengaged to form higher size of bubbles and for this reason the two nozzles do not show appreciable increase in their average diameter.

6.5. *Path Lines.* Figure 24 represents the path lines of liquid for nozzles 1, 3, and 5, respectively. It is evident from the figure

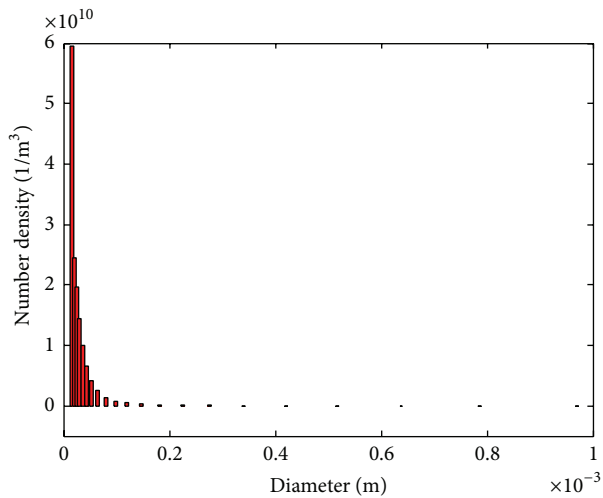


FIGURE 15: Plot of the number density of bubble in the entire volume for nozzle 1.

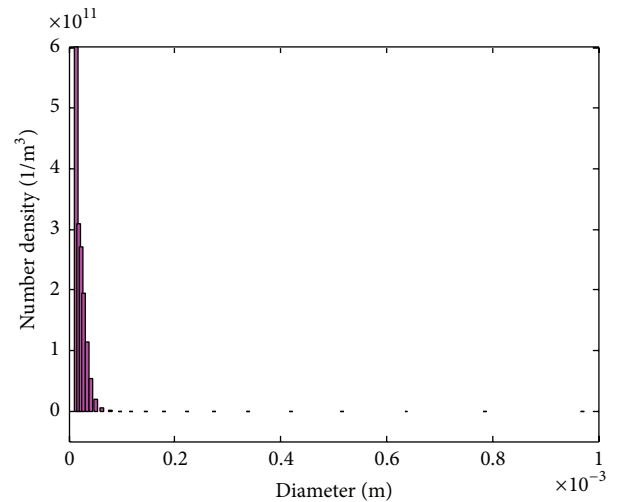


FIGURE 18: Plot of the number density of bubble in a plane near to the gas inlet for nozzle 1.

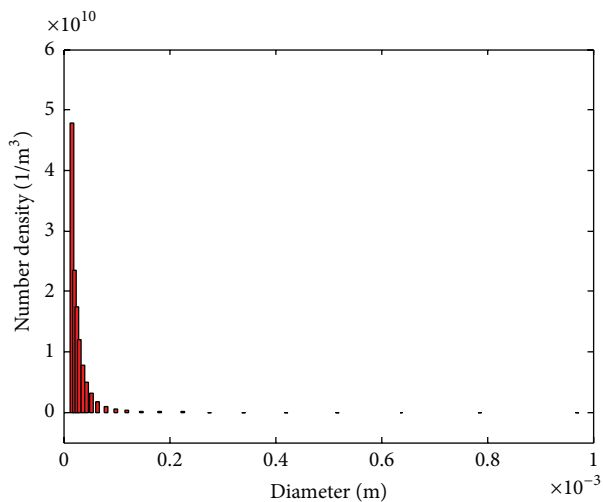


FIGURE 16: Plot of the number density of bubble in the entire volume for nozzle 3.

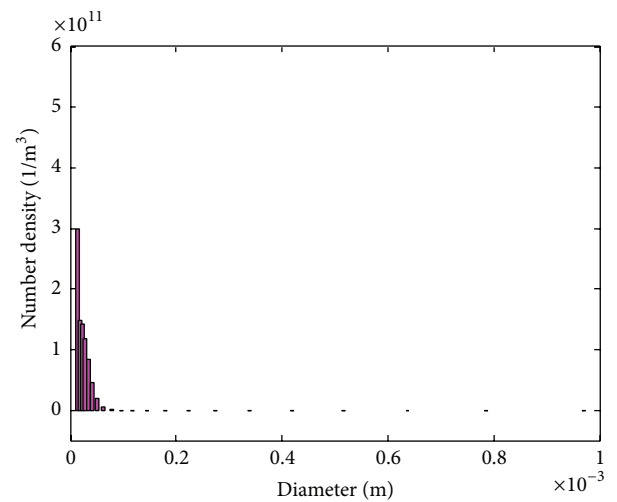


FIGURE 19: Plot of the number density of bubble in a plane near to the gas inlet for nozzle 3.

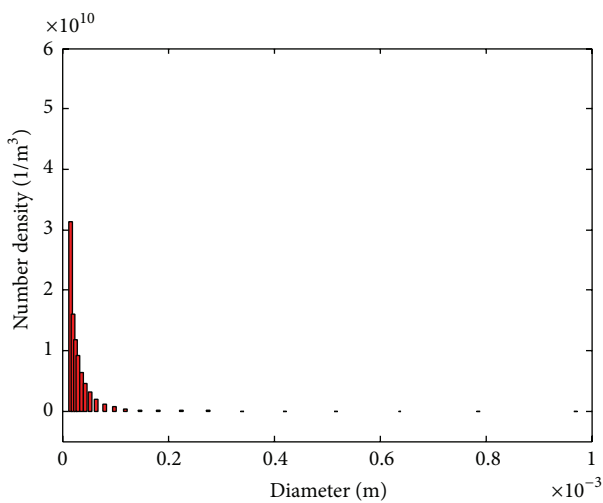


FIGURE 17: Plot of the number density of bubble in the entire volume for nozzle 5.

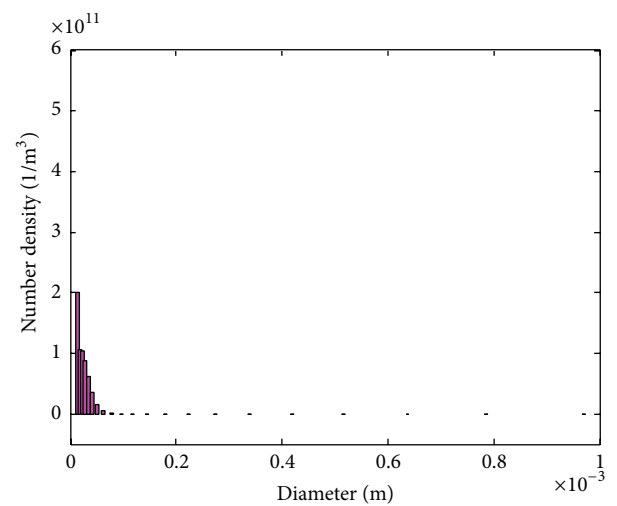


FIGURE 20: Plot of the number density of bubble in a plane near to the gas inlet for nozzle 5.

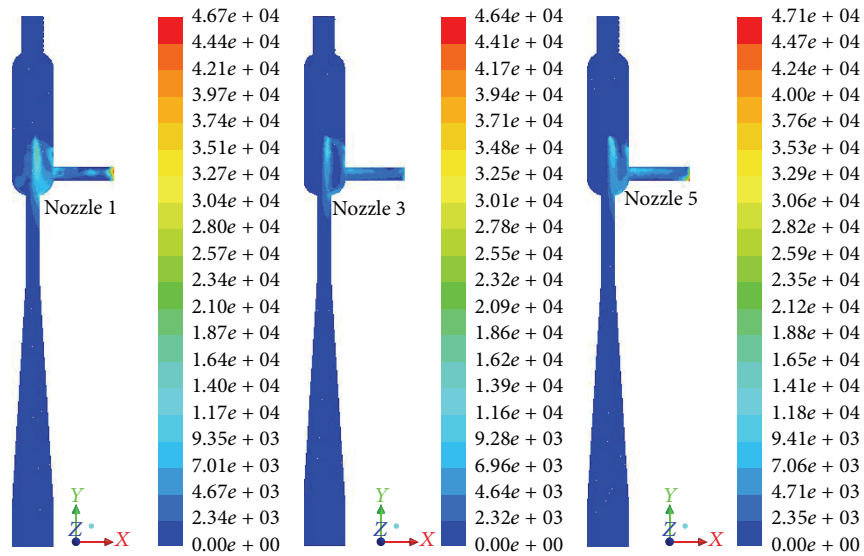


FIGURE 21: Contour of the interfacial area on middle plane for nozzles 1, 3, and 5.

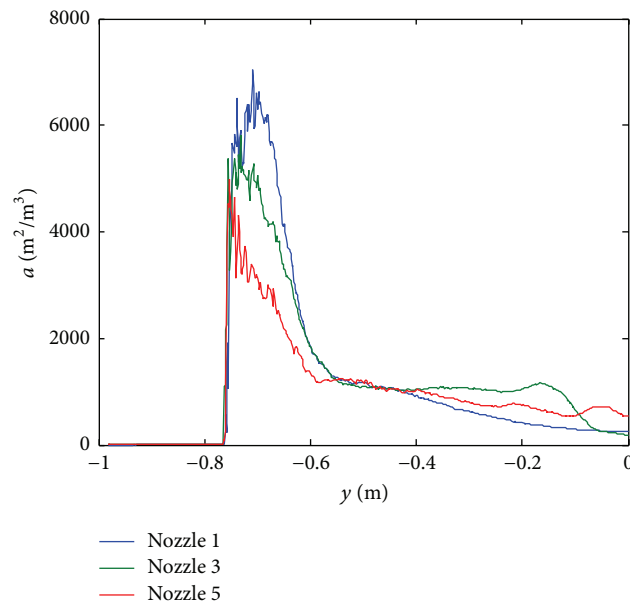


FIGURE 22: Plot of the interfacial area.

that larger recirculation region occurs in the mixing as the number of nozzles increases.

## 7. Conclusion

Population balance approach, combined with the coalescence and break-up models, is presented to simulate the operation of the jet ejector, using CFD software. The population balance approach was demonstrated by using the equation of bubble number density for gas-liquid flows using *ANSYS Fluent 14.0* to explain the temporal and spatial changes of the gas bubble size distribution. The CFD results have been analyzed to determine bubble size distribution, liquid velocity, gas velocity, and volume fraction in the jet ejector with the  $\text{Cl}_2\text{-NaOH}$  system. Computational results are

compared with the experimental results [31]. The simulated interfacial area is in good agreement with the experimental values.

In order to see the validity of the CFD model we require more experimental data on liquid-to-gas ratio, geometry of the jet ejector, properties of gas and liquid, reactivity of fluids, and so forth. The coupling of all these properties gives a good platform to predict the best model and as a consequence we may predict the performance of the jet ejector.

## Conflict of Interests

The authors declare that there is no conflict of interests regarding the publication of this paper.

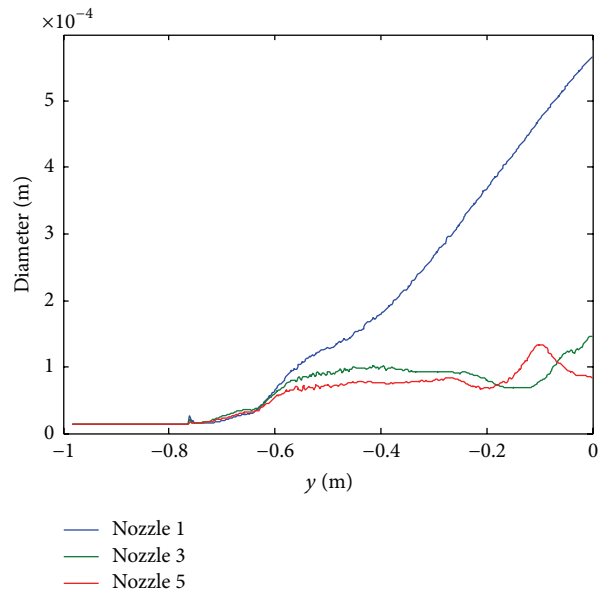


FIGURE 23: Plot of the diameter of bubble.

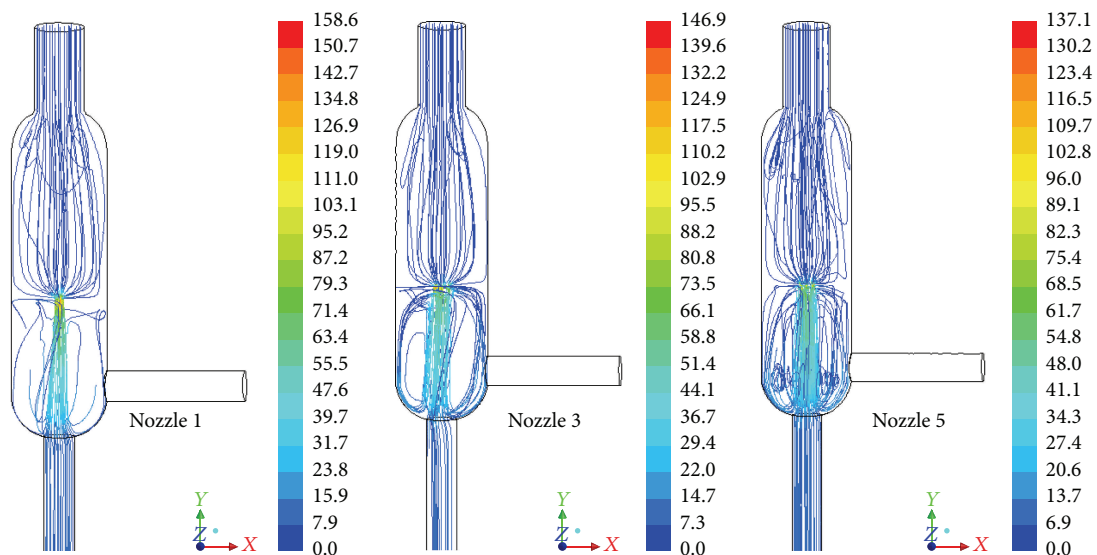


FIGURE 24: Path lines of liquid for nozzles 1, 3, and 5.

## Acknowledgment

The first author gratefully acknowledges the financial support received from Department of Mathematics and Physics, Lappeenranta University of Technology, Lappeenranta, Finland, for international mobility support, making this joint research work possible.

## References

- [1] K. Ekambara, R. Sean Sanders, K. Nandakumar, and J. H. Masliyah, "CFD modeling of gas-liquid bubbly flow in horizontal pipes: influence of bubble coalescence and breakup," *International Journal of Chemical Engineering*, vol. 2012, Article ID 620463, 20 pages, 2012.
- [2] E. Olmos, C. Gentric, C. Vial, G. Wild, and N. Midoux, "Numerical simulation of multiphase flow in bubble column reactors. Influence of bubble coalescence and break-up," *Chemical Engineering Science*, vol. 56, no. 21-22, pp. 6359–6365, 2001.
- [3] K. A. Mouza, N. A. Kazakis, and S. V. Paras, "Bubble column reactor design using a CFD code," in *Proceedings of the 1st International Conference "From Scientific Computing to Computational Engineering" (IC-SCCE '04)*, Athens, Greece, September 2004.
- [4] J. B. Joshi, V. S. Vitankar, A. A. Kulkarni, M. T. Dhotre, and K. Ekambara, "Coherent flow structures in bubble column reactors," *Chemical Engineering Science*, vol. 57, no. 16, pp. 3157–3183, 2002.
- [5] G. Kocamustafaogullari and W. D. Huang, "Internal structure and interfacial velocity development for bubbly two-phase

- flow,” *Nuclear Engineering and Design*, vol. 151, no. 1, pp. 79–101, 1994.
- [6] A. Kitagawa, K. Sugiyama, and Y. Murai, “Experimental detection of bubble-bubble interactions in a wall-sliding bubble swarm,” *International Journal of Multiphase Flow*, vol. 30, no. 10, pp. 1213–1234, 2004.
- [7] G. Wild, S. Poncin, H. Li, and E. Olmos, “Some aspects of the hydrodynamics of bubble columns,” *International Journal of Chemical Reactor Engineering*, vol. 1, no. 1, pp. 1–36, 2003.
- [8] W.-D. Deckwer, *Bubble Column Reactors*, John Wiley & Sons, Chichester, UK, 1992.
- [9] P. Spicka, M. M. Dias, and J. C. B. Lopes, “Gas-liquid flow in a 2D column: comparison between experimental data and CFD modelling,” *Chemical Engineering Science*, vol. 56, no. 21–22, pp. 6367–6383, 2001.
- [10] J. Cao and R. N. Christensen, “Analysis of moving boundary problem for bubble collapse in binary solutions,” *Numerical Heat Transfer, Part A: Applications*, vol. 38, no. 7, pp. 681–699, 2000.
- [11] R. D. S. Cavalcanti, S. R. De Farias Neto, and E. O. Vilar, “A computational fluid dynamics study of hydrogen bubbles in an electrochemical reactor,” *Brazilian Archives of Biology and Technology*, vol. 48, pp. 219–229, 2005.
- [12] R. Krishna and J. M. Van Baten, “Scaling up bubble column reactors with the aid of CFD,” *Chemical Engineering Research and Design*, vol. 79, no. 3, pp. 283–309, 2001.
- [13] J. M. Van Baten and R. Krishna, “Scale up studies on partitioned bubble column reactors with the aid of CFD simulations,” *Catalysis Today*, vol. 79–80, pp. 219–227, 2003.
- [14] K. Shimizu, S. Takada, K. Minekawa, and Y. Kawase, “Phenomenological model for bubble column reactors: prediction of gas hold-ups and volumetric mass transfer coefficients,” *Chemical Engineering Journal*, vol. 78, no. 1, pp. 21–28, 2000.
- [15] V. V. Buwa and V. V. Ranade, “Dynamics of gas-liquid flow in a rectangular bubble column: experiments and single/multi-group CFD simulations,” *Chemical Engineering Science*, vol. 57, no. 22–23, pp. 4715–4736, 2002.
- [16] S. Lo, “Application of population balance to CFD modelling of gas-liquid reactors,” in *Proceedings of the Conference on Trends in Numerical and Physical Modelling for Industrial Multiphase Flows*, Cargèse, France, September 2000.
- [17] M. T. Dhotre, K. Ekambara, and J. B. Joshi, “CFD simulation of sparger design and height to diameter ratio on gas hold-up profiles in bubble column reactors,” *Experimental Thermal and Fluid Science*, vol. 28, no. 5, pp. 407–421, 2004.
- [18] J.-M. Delhay and J. B. McLaughlin, “Appendix 4: report of study group on microphysics,” *International Journal of Multiphase Flow*, vol. 29, no. 7, pp. 1101–1116, 2003.
- [19] M. J. Prince and H. W. Blanch, “Bubble coalescence and breakup in air-sparged bubble columns,” *AIChE Journal*, vol. 36, no. 10, pp. 1485–1499, 1990.
- [20] J. Y. Tu, G. H. Yeoh, G.-C. Park, and M.-O. Kim, “On population balance approach for subcooled boiling flow prediction,” *Journal of Heat Transfer*, vol. 127, no. 3, pp. 253–264, 2005.
- [21] T. Wang, J. Wang, and Y. Jin, “A novel theoretical breakup kernel function for bubbles/droplets in a turbulent flow,” *Chemical Engineering Science*, vol. 58, no. 20, pp. 4629–4637, 2003.
- [22] T. Wang, J. Wang, and Y. Jin, “A CFD-PBM coupled model for gas-liquid flows,” *AIChE Journal*, vol. 52, no. 1, pp. 125–140, 2006.
- [23] J. Hämäläinen, S. B. Lindström, T. Hämäläinen, and H. Niskanen, “Papermaking fibre-suspension flow simulations at multiple scales,” *Journal of Engineering Mathematics*, vol. 71, no. 1, pp. 55–79, 2011.
- [24] T. Hämäläinen, *Modelling of fibre orientation and fibre flocculation phenomena in paper sheet forming [Ph.D. thesis]*, Tampere University of Technology, Publication 768, Tampere, Finland, 2008.
- [25] F. Lehr, M. Millies, and D. Mewes, “Bubble-size distributions and flow fields in bubble columns,” *AIChE Journal*, vol. 48, no. 11, pp. 2426–2443, 2002.
- [26] F. B. Campos and P. L. C. Lage, “A numerical method for solving the transient multidimensional population balance equation using an Euler-Lagrange formulation,” *Chemical Engineering Science*, vol. 58, no. 12, pp. 2725–2744, 2003.
- [27] P. Chen, J. Sanyal, and M. P. Dudukovic, “CFD modeling of bubble columns flows: implementation of population balance,” *Chemical Engineering Science*, vol. 59, no. 22–23, pp. 5201–5207, 2004.
- [28] H. Luo and H. F. Svendsen, “Theoretical model for drop and bubble breakup in turbulent dispersions,” *AIChE Journal*, vol. 42, no. 5, pp. 1225–1233, 1996.
- [29] G. H. Yeoh and J. Y. Tu, “Population balance modelling for bubbly flows with heat and mass transfer,” *Chemical Engineering Science*, vol. 59, no. 15, pp. 3125–3139, 2004.
- [30] I. Atay, *Fluid flow and gas absorption, in an ejector venturiscrubber [Dissertation for the Degree of Doctor of Engineering Science]*, New Jersey Institute of Technology, Newark, NJ, USA, 1986.
- [31] K. S. Agrawal, *Modeling of multi nozzle jet ejector for absorption with chemical reaction [Doctor of Philosophy Thesis in Chemical Engineering]*, Maharaja Sayajirao University of Baroda, Vadodara, India, 2012.
- [32] K. S. Agrawal, “Jet ejector and its importance in context of Indian industry,” *International Journal of Applied Environmental Sciences*, vol. 8, no. 3, pp. 267–269, 2013.
- [33] A. Laurent and J. C. Charpentier, “Aires interfaciales et coefficients de transfert de matière dans les divers types d’absorbants et de réacteurs gaz-liquide,” *The Chemical Engineering Journal*, vol. 8, no. 2, pp. 85–101, 1974.
- [34] M. Zlokarnik, “Eignung und leistungsfähigkeit von belüftungs-vorrichtungen für die biologische abwasserreinigung,” *Chemie Ingenieur Technik*, vol. 52, no. 4, pp. 330–331, 1980.
- [35] S. Ogawa, H. Yamaguchi, S. Tone, and T. Otake, “Gas-liquid mass transfer in the jet reactor with liquid jet reactor,” *Journal of Chemical Engineering of Japan*, vol. 16, no. 5, pp. 419–425, 1983.
- [36] J. C. Charpentier, “What’s new in absorption with chemical reaction?” *Transactions of the Institution of Chemical Engineers*, vol. 60, pp. 131–156, 1982.
- [37] M. A. M. Costa, A. P. R. A. Ribeiro, É. R. Tognetti, M. L. Aguiar, J. A. S. Gonçalves, and J. R. Coury, “Performance of a Venturi scrubber in the removal of fine powder from a confined gas stream,” *Materials Research*, vol. 8, no. 2, pp. 177–179, 2005.
- [38] A. Majid, Y. C. Qi, and K. Mehboob, “A review of performance of a venturi scrubber,” *Research Journal of Applied Sciences, Engineering and Technology*, vol. 4, no. 19, pp. 3811–3818, 2012.
- [39] T. Utomo, Z. Jin, M. Rahman, H. Jeong, and H. Chung, “Investigation on hydrodynamics and mass transfer characteristics of a gas-liquid ejector using three-dimensional CFD modeling,” *Journal of Mechanical Science and Technology*, vol. 22, no. 9, pp. 1821–1829, 2008.

- [40] S. K. Das and M. N. Biswas, "Studies on ejector-venturi fume scrubber," *Chemical Engineering Journal*, vol. 119, no. 2-3, pp. 153-160, 2006.
- [41] D. Li, *Investigation of an ejector-expansion device in a transcritical carbon dioxide cycle for military ECU applications [Ph.D. thesis]*, Purdue University, West Lafayette, Ind, USA, 2006.
- [42] J. H. Witte, "Mixing shocks in two-phase flow," *Journal of Fluid Mechanics*, vol. 36, no. 4, pp. 639-655, 1969.
- [43] R. L. Yadav and A. W. Patwardhan, "Design aspects of ejectors: effects of suction chamber geometry," *Chemical Engineering Science*, vol. 63, no. 15, pp. 3886-3897, 2008.
- [44] H. Blenke, K. Bohner, and E. Vollmerhaus, "Untersuchungen zur berechnung des betriebsverhaltens von treibstrahlförderern," *Chemie Ingenieur Technik*, vol. 35, no. 3, pp. 201-208, 1963.
- [45] S. T. Bonnington, "Water jet ejectors," BHRA Publication RR540, 1956.
- [46] S. T. Bonnington, "Water driven air ejectors," Tech. Rep. SP664, BHRA Publication, 1960.
- [47] S. T. Bonnington, "A guide to jet pump design," *British Chemical Engineering*, vol. 9, no. 3, pp. 150-154, 1964.
- [48] S. T. Bonnington and A. L. King, *Jet Pumps and Ejectors: A State of the Art Review and Bibliography*, BHRA Fluid Engineering, Bedford, UK, 1972.
- [49] R. G. Cunningham, "Gas compression with the liquid jet pump," *Journal of Fluids Engineering*, vol. 96, no. 3, pp. 203-215, 1974.
- [50] R. G. Cunningham and R. J. Dopkin, "Jet breakup and mixing throat lengths for the liquid jet gas pump," *Transactions of the ASME, Journal of Fluids Engineering*, vol. 96, no. 3, pp. 216-226, 1974.
- [51] X. Gamisans, M. Sarrà, and F. J. Lafuente, "The role of the liquid film on the mass transfer in venturi-based scrubbers," *Chemical Engineering Research and Design*, vol. 82, no. 3, pp. 372-380, 2004.
- [52] G. C. Govatos, "The slurry pump," *Journal of Pipelines*, vol. 1, pp. 145-157, 1981.
- [53] A. E. Kroll, "The design of jet pump," *Chemical Engineering Progress*, vol. 43, no. 2, pp. 21-24, 1947.
- [54] D. K. Acharjee, P. A. Bhat, A. K. Mitra, and N. A. Roy, "Studies on momentum transfer in vertical liquid jet ejectors," *Indian Journal of Technology*, vol. 13, pp. 205-210, 1975.
- [55] P. A. Bhat, A. K. Mitra, and A. N. Roy, "Momentum transfer in a horizontal liquid-jet ejector," *The Canadian Journal of Chemical Engineering*, vol. 50, no. 3, pp. 313-317, 1972.
- [56] M. N. Biswas, A. K. Mitra, and A. N. Roy, "Effective interfacial area in a liquid-jet induced horizontal gas-liquid pipeline contactor," *Indian Chemical Engineer*, vol. 19, no. 2, pp. 15-21, 1977.
- [57] M. N. Biswas, A. K. Mitra, and A. N. Roy, "Studies on gas dispersion in a horizontal liquid jet ejector," in *Proceedings of the 2nd Symposium on Jet Pumps and Ejectors and Gas Lift Techniques*, E3-27-42, BHRA, Cambridge, UK, March 1975.
- [58] W. J. Davis, "The effect of the Froude number in estimating vertical 2-phase gas-liquid friction losses," *British Chemical Engineering*, vol. 8, pp. 462-465, 1963.
- [59] G. S. Davles, A. K. Mitra, and A. N. Roy, "Momentum transfer studies in ejectors. Correlations for single-phase and two-phase systems," *Industrial & Engineering Chemistry Process Design and Development*, vol. 6, no. 3, pp. 293-299, 1967.
- [60] X. Gamisans, M. Sarrà, and F. J. Lafuente, "Gas pollutants removal in a single- and two-stage ejector-venturi scrubber," *Journal of Hazardous Materials*, vol. 90, no. 3, pp. 251-266, 2002.
- [61] S. Dasappa, P. J. Paul, and H. J. Mukunda, "Fluid dynamic studies on ejectors for thermal applications of gasifiers," in *Proceedings of the 4th National Meet on Recent Advances in Biomass Gasification Technology*, Mysore, India, 1993.
- [62] A. K. Mitra and A. N. Roy, "Studies on the performance of ejector: correlation for air-air system," *Indian Journal of Technology*, vol. 2, no. 9, pp. 315-316, 1964.
- [63] A. K. Mitra, D. K. Guha, and A. N. Roy, "Studies on the performance of ejector Part-I, air-air system," *Indian Chemical Engineering Transactions*, vol. 5, article 59, 1963.
- [64] D. Mukherjee, M. N. Biswas, and A. K. Mitra, *Holdup Studies in Liquid; Liquid Ejector System*, vol. 1, Institute of Chemical Engineers, 1981.
- [65] D. Mukherjee, M. N. Biswas, and A. K. Mitra, "Hydrodynamics of liquid-liquid dispersion in ejectors and vertical two phase flow," *Canadian Journal of Chemical Engineering*, vol. 66, no. 6, pp. 896-907, 1988.
- [66] V. R. Radhakrishnan and A. K. Mitra, "Pressure drop, holdup and interfacial area in vertical two-phase flow of multi-jet ejector induced dispersions," *Canadian Journal of Chemical Engineering*, vol. 62, no. 2, pp. 170-178, 1984.
- [67] S. S. Pal, A. K. Mitra, and A. N. Roy, "Pressure drop and holdup in a vertical two-phase counter current flow with improved gas mixing liquid," *Industrial & Engineering Chemistry Process Design and Development*, vol. 19, no. 1, pp. 67-75, 1979.
- [68] K. P. Singh, N. K. Purohit, and A. K. Mitra, "Performance characteristics of a horizontal ejector: water-water system," *Indian Chemical Engineer*, vol. 16, no. 3, pp. 1-6, 1974.
- [69] K. S. Agrawal, "Performance of venturi scrubber," *International Journal of Engineering Research and Development*, vol. 7, no. 11, pp. 53-69, 2013.
- [70] K. S. Agrawal, "Interfacial area and mass transfer characteristics in multi nozzle jet ejector," *International Journal of Emerging Technologies in Computational and Applied Sciences*, vol. 3, no. 5, pp. 270-280, 2013.
- [71] S. K. Agrawal, "Bubble dynamics and interface phenomenon," *Journal of Engineering and Technology Research*, vol. 5, no. 3, pp. 42-50, 2013.
- [72] S. Balamurugan, M. D. Lad, V. G. Gaikar, and A. W. Patwardhan, "Effect of geometry on mass transfer characteristics of ejectors," *Industrial and Engineering Chemistry Research*, vol. 46, no. 25, pp. 8505-8517, 2007.
- [73] S. Balamurugan, V. G. Gaikar, and A. W. Patwardhan, "Effect of ejector configuration on hydrodynamic characteristics of gas-liquid ejectors," *Chemical Engineering Science*, vol. 63, no. 3, pp. 721-731, 2008.
- [74] N. N. Dutta and K. V. Raghavan, "Mass transfer and hydrodynamic characteristics of loop reactors with downflow liquid jet ejector," *The Chemical Engineering Journal*, vol. 36, no. 2, pp. 111-121, 1987.
- [75] P. Havelka, V. Linek, J. Sinkule, J. Zahradník, and M. Fialová, "Hydrodynamic and mass transfer characteristics of ejector loop reactors," *Chemical Engineering Science*, vol. 55, no. 3, pp. 535-549, 2000.
- [76] P. Havelka, V. Linek, J. Sinkule, J. Zahradník, and M. Fialová, "Effect of the ejector configuration on the gas suction rate and gas hold-up in ejector loop reactors," *Chemical Engineering Science*, vol. 52, no. 11, pp. 1701-1713, 1997.
- [77] C. Li and Y. Z. Li, "Investigation of entrainment behavior and characteristics of gas-liquid ejectors based on CFD simulation," *Chemical Engineering Science*, vol. 66, no. 3, pp. 405-416, 2011.

- [78] A. Mandal, "Characterization of gas-liquid parameters in a down-flow jet loop bubble column," *Brazilian Journal of Chemical Engineering*, vol. 27, no. 2, pp. 253–264, 2010.
- [79] A. Mandal, G. Kundu, and D. Mukherjee, "Gas-holdup distribution and energy dissipation in an ejector-induced downflow bubble column: the case of non-Newtonian liquid," *Chemical Engineering Science*, vol. 59, no. 13, pp. 2705–2713, 2004.
- [80] A. Mandal, G. Kundu, and D. Mukherjee, "Interfacial area and liquid-side volumetric mass transfer coefficient in a downflow bubble column," *Canadian Journal of Chemical Engineering*, vol. 81, no. 2, pp. 212–219, 2003.
- [81] A. Mandal, G. Kundu, and D. Mukherjee, "Gas holdup and entrainment characteristics in a modified downflow bubble column with Newtonian and non-Newtonian liquid," *Chemical Engineering and Processing: Process Intensification*, vol. 42, no. 10, pp. 777–787, 2003.
- [82] A. Mandal, G. Kundu, and D. Mukherjee, "A comparative study of gas holdup, bubble size distribution and interfacial area in a downflow bubble column," *Chemical Engineering Research and Design*, vol. 83, no. 4, pp. 423–428, 2005.
- [83] A. Mandal, G. Kundu, and D. Mukherjee, "Energy analysis and air entrainment in an ejector induced downflow bubble column with non-Newtonian motive fluid," *Chemical Engineering & Technology*, vol. 28, no. 2, pp. 210–218, 2005.
- [84] D. A. Mitchell, "Improving the efficiency of free-jet scrubbers," *Environment International*, vol. 6, no. 1–6, pp. 21–24, 1981.
- [85] F. Rahman, D. B. Umesh, D. Subbarao, and M. Ramasamy, "Enhancement of entrainment rates in liquid-gas ejectors," *Chemical Engineering and Processing: Process Intensification*, vol. 49, no. 10, pp. 1128–1135, 2010.
- [86] W. Yaici, A. Laurent, N. Midoux, and J.-C. Charpentier, "Determination of gas-side mass transfer coefficients in trickle-bed reactors in the presence of an aqueous or an organic liquid phase," *International Chemical Engineering*, vol. 28, no. 2, pp. 299–305, 1988.
- [87] K. Yamagiwa, D. Kusabiraki, and A. Ohkawa, "Gas holdup and gas entrainment rate in downflow bubble column with gas entrainment by a liquid jet operating at high liquid throughput," *Journal of Chemical Engineering of Japan*, vol. 23, no. 3, pp. 343–348, 1990.
- [88] T. Frank, "Advances in computational fluid dynamics (CFD) of 3-dimensional gas-liquid multiphase flows," in *Proceedings of the NAFEMS Seminar: Simulation of Complex Flows (CFD)*, Niedernhausen/Wiesbaden, Germany, April 2005.
- [89] A. A. Kendoush and S. A. W. Al-khatib, "Flow regimes characterization in vertical downward two phase flow," in *Proceedings of the 2nd International Symposium on Multiphase Flow and Heat Transfer*, X. Z. Chen, T. N. Veziroglu, and C. L. Tien, Eds., pp. 215–220, 1989.
- [90] J. Zahradník and M. Fialová, "The effect of bubbling regime on gas and liquid phase mixing in bubble column reactors," *Chemical Engineering Science*, vol. 51, no. 10, pp. 2491–2500, 1996.
- [91] R. G. Rice and M. A. Littlefield, "Dispersion coefficients for ideal bubbly flow in truly vertical bubble columns," *Chemical Engineering Science*, vol. 42, no. 8, pp. 2045–2053, 1987.
- [92] B. R. Bakshi, P. Jiang, and L. S. Fan, "Analysis of flow in gas-liquid bubble columns using multi-resolution methods," in *Proceedings of the 2nd International Conference on Gas-Liquid-Solid Reactor Engineering*, pp. A1–A8, Cambridge, Mass, USA, March 1995.
- [93] H. Lefebvre, *Atomization and Sprays*, Hemisphere Publishing Corporation, New York, NY, USA, 1989.
- [94] H. Liu, *Science and Engineering of Droplets: Fundamentals and Applications*, Noyes Publications, New York, NY, USA, 2000.
- [95] R. J. Schick, "Spray technology reference guide: understanding drop size," Bulletin 4598, Spraying Systems, Wheaton, Ill, USA, 2006.
- [96] L. Xianguo and R. S. Tankin, "Droplet size distribution: a derivative of a Nukiyama—Tanasawa type distribution function," *Combustion Science and Technology*, vol. 56, no. 1, pp. 65–76, 1987.
- [97] A. Dennis Gary, "A study of injector spray characteristics in simulated rocket combustion chamber including longitudinal mode pressure oscillation," Tech. Rep. 730, NASA, 1966.
- [98] M. Azad and S. R. Syeda, "A numerical model for bubble size distribution in turbulent gas-liquid dispersion," *Journal of Chemical Engineering*, vol. 24, no. 1, pp. 25–34, 2006.
- [99] M. K. Silva, M. A. D. Ávila, and M. Mori, "CFD modelling of a bubble column with an external loop in the heterogeneous regime," *The Canadian Journal of Chemical Engineering*, vol. 89, no. 4, pp. 671–681, 2011.
- [100] A. N. Kudzo, *Visualization and characterization of ultrasonic cavitating atomizer and other automotive paint sprayers using infrared thermography [A Dissertation Submitted in Partial Fulfillment of the Requirements for the Degree of Doctor of Philosophy]*, College of Engineering, University of Kentucky, Lexington, Ky, USA, 2009.
- [101] J. Ciborowski and A. Bin, "Investigation of the aeration effect of plunging liquid jets," *Inzynieria Chemiczna*, vol. 2, pp. 557–577, 1972.
- [102] A. Ohkawa, D. Kusabiraki, Y. Kawai, N. Sakai, and K. Endoh, "Some flow characteristics of a vertical liquid jet system having downcomers," *Chemical Engineering Science*, vol. 41, no. 9, pp. 2347–2361, 1986.
- [103] Y. Y. Sheng and G. A. Irons, "The impact of bubble dynamics on the flow in plumes of ladle water models," *Metallurgical and Materials Transactions B*, vol. 26, no. 3, pp. 625–635, 1995.
- [104] J. Kitscha and G. Kocamustafaogullari, "Breakup criteria for fluid particles," *International Journal of Multiphase Flow*, vol. 15, no. 4, pp. 573–588, 1989.
- [105] F. O. Bailer, *Mass transfer characteristics of a novel gas-liquid contactor, the advanced buss loop reactor [A Dissertation Submitted to the Swiss Federal Institute of Technology for Degree of Doctor of Technical Sciences]*, Swiss Federal Institute of Technology, Zürich, Switzerland, 2001.
- [106] G. M. Evans, G. J. Jameson, and B. W. Atkinson, "Prediction of the bubble size generated by a plunging liquid jet bubble column," *Chemical Engineering Science*, vol. 47, no. 13–14, pp. 3265–3272, 1992.
- [107] K. Ceylan, A. Altunbaş, and G. Kelbaliyev, "A new model for estimation of drag force in the flow of Newtonian fluids around rigid or deformable particles," *Powder Technology*, vol. 119, no. 2–3, pp. 250–256, 2001.
- [108] R. Pawelczyk and K. Pindur, "A dynamic method for dispersing gases in liquids," *Chemical Engineering and Processing: Process Intensification*, vol. 38, no. 2, pp. 95–107, 1999.
- [109] A. K. Biń, "Gas entrainment by plunging liquid jets," *Chemical Engineering Science*, vol. 48, no. 21, pp. 3585–3630, 1993.
- [110] S.-Q. Zheng, Y. Yao, F.-F. Guo, R.-S. Bi, and J.-Y. Li, "Local bubble size distribution, gas-liquid interfacial areas and gas holdups in an up-flow ejector," *Chemical Engineering Science*, vol. 65, no. 18, pp. 5264–5271, 2010.

- [111] K. S. Agrawal, "Removal efficiency in industrial scale liquid jet ejector for chlorine-aqueous caustic soda system," *International Journal of Engineering Trends and Technology*, vol. 4, no. 7, pp. 2931–2940, 2013.
- [112] K. S. Agrawal, "Experimental observation for liquid jet ejector for chlorine-aqueous caustic soda system at laboratory scale," *American International Journal of Research in Science, Technology, Engineering and Mathematics*, vol. 2, no. 2, pp. 177–181, 2013.
- [113] K. S. Agrawal, "Performance of venturi scrubber," *International Journal of Engineering Research and Development*, vol. 17, no. 11, pp. 53–69, 2013.
- [114] N. A. Panchal, S. R. Bhutada, and V. G. Pangarkar, "Gas induction and hold up characteristics of liquid jet loop reactor using multi orifice nozzles," *Chemical Engineering Communications*, vol. 102, no. 1, pp. 59–68, 1991.